Calculation of the crystal-field parameters, electric field gradient and magnetic moments in $PrNi_5$

1993 J. Phys.: Condens. Matter 5 8417

(http://iopscience.iop.org/0953-8984/5/44/027)

J. Phys.: Condens. Matter 5 (1993) 8417–8424. Printed in the UK

Calculation of the crystal-field parameters, electric field gradient and magnetic moments in $PrNi_5$

J Kuriplach† and P Novák‡

† Faculty of Mathematics and Physics, Charles University, V Holešovičkách 2, 180 00 Prague 8, Czech Republic

‡ Institute of Physics, Cukrovarnická 10, 162 00 Prague 6, Czech Republic

Received 14 June 1993, in final form 2 August 1993

Abstract. The electronic structure of $PrNi_5$ was calculated using the full potential LAPW method. On this basis the crystal-field parameters were determined and compared with experimental results. The electric field gradient at the Pr nucleus site was also calculated. The problem of the existence of Ni magnetic moments is challenged.

1. Introduction

To explain the magnetocrystalline anisotropy of the intermetallic rare earth compounds, semiempirical models that incorporate crystal-field effects are used as a rule. Corresponding calculations meet with serious difficulties, however, as in most cases little is known about the crystal-field parameters (CFPs) that enter the models. Recently there have been several attempts to determine CFPs on the basis of *ab initio* electronic structure calculation [1–7]. Again, however, the difficulty appears when the calculated parameters are confronted with the experimental results—in most cases an uncertainty exists in the values of the 'experimental' CFPs determined by fitting the selected experimental results. In this respect $PrNi_5$ represents an exception—because of its importance as a material for adiabatic demagnetization, it has been studied many times; in particular CFPs have been determined by several investigators and reliable data are now available (see [8] and references therein). For this reason we decided to calculate CFPs for this compound by an *ab initio* method.

When interpreting experiments on $PrNi_5$ the question about Ni magnetic moments often appears. For instance in the recent experiment [8], where the technique of inelastic neutron scattering was used, the workers showed that experimental data can be explained supposing that Ni atoms have no moments. Within the accuracy of that experiment the dispersion of the $\Gamma_4 \rightarrow \Gamma_5^{(1)}$ transition with the scattering vector is examined as the effect of exchange interaction. At present, it is clear that the Ni 3d shell is practically filled, but there is some space for small magnetic moments of Ni.

The strength of electric quadrupole hyperfine interaction at the Pr nucleus site was also measured [9]. There are several contributions to the electric field gradient (EFG) and it is difficult to distinguish between them in experiments. We would also like to contribute to the solution of this problem.

0953-8984/93/448417+08$07.50

2. Electronic structure calculation

To study anisotropic properties of crystals (crystal field, electric field gradient) full potential methods should preferably be used. We employed the full potential linearized augmented plane wave (FLAPW) method and the package of programs developed by Blaha *et al* [10], which we modified slightly. In this method there are no restrictions of the shape of the potential (or density)—no averaging is performed. A crystal is divided into two regions:

(i) the muffin-tin region, which is compounded by non-overlaping spheres centred at nuclear sites; and

(ii) the region outside these spheres—i.e., the interstitial region.

The potential is expanded inside the muffin-tin spheres into the spherical harmonics:

$$V(r) = \sum_{L,M} V_{LM}(r) Y_{LM}(\theta, \varphi). \tag{1}$$

In the interstitial region, the plane wave representation of the potential is used so that the potential is continuous on the muffin-tin boundary. Analogously the electronic density is also expanded.

$PrNi_5$ crystallizes in the hexagonal $CaCu_5$ structure with lattice parameters $a = 9.369$ au and $c = 7.521$ au [11]. These parameters were used in our calculation.

As is usual in the LAPW method, we divided electronic states into several types: valence (6s, 5d, 6p for Pr and 4s, 3d, 4p for Ni); semi-core (5s, 5p for Pr, none for Ni); 4f semi-core [4] (4f for Pr). Remaining states are treated as the core states. For 4f semi-core states, electronic energies were calculated only in the Γ point to avoid delocalization of 4f electrons [4].

We performed both spin-polarized and non-spin-polarized calculations, denoted hereafter as SP and NSP, respectively. The exchange–correlation potential as described in [12] for the SP case was used. Analogously in the NSP case the potential from [13] was taken. In the SP case we have found two different self-consistent solutions: for solution A, Ni moments were antiparallel to Pr moments, while for B, parallel orientation of Ni and Pr moments was obtained (for a discussion of the values of these moments see below). We have also obtained another self-consistent solution (using another set of lattice parameters) and results are discussed elsewhere [14].

Scalar relativistic corrections were included when calculating the energies and wave functions of valence and (4f) semi-core electrons. Core electrons were treated fully relativistically.

We should mention our difficulties during the self-consistent cycle. These problems seem to be similar to those discussed by Schwarz and Mohn [15] and seem to originate from the flat dependence of the total energy on magnetization. In such cases many iterations are needed to achieve self-consistency even if a sophisticated mixing scheme [10] is used. To avoid convergency problems the fixed spin moment method (see, e.g., [15]) should be used. The level of self-consistency achieved in our calculations is characterized by the change of the following quantities in two subsequent iterations: total energy < 1 mRyd and valence charges in muffin-tin spheres $< 0.005e$.

Figure 1 shows the valence density of states (DOS) for majority and minority spins for the SP-B case. We can see that the shape of DOS curves for both spins is very similar and that these curves are mutually slightly shifted. States around the main peak (~ 0.55 Ryd) have dominantly 3d character and originate from 3d states of Ni. The nickel 3d band is nearly filled, as is obvious from the position of the Fermi level. Small peaks higher in

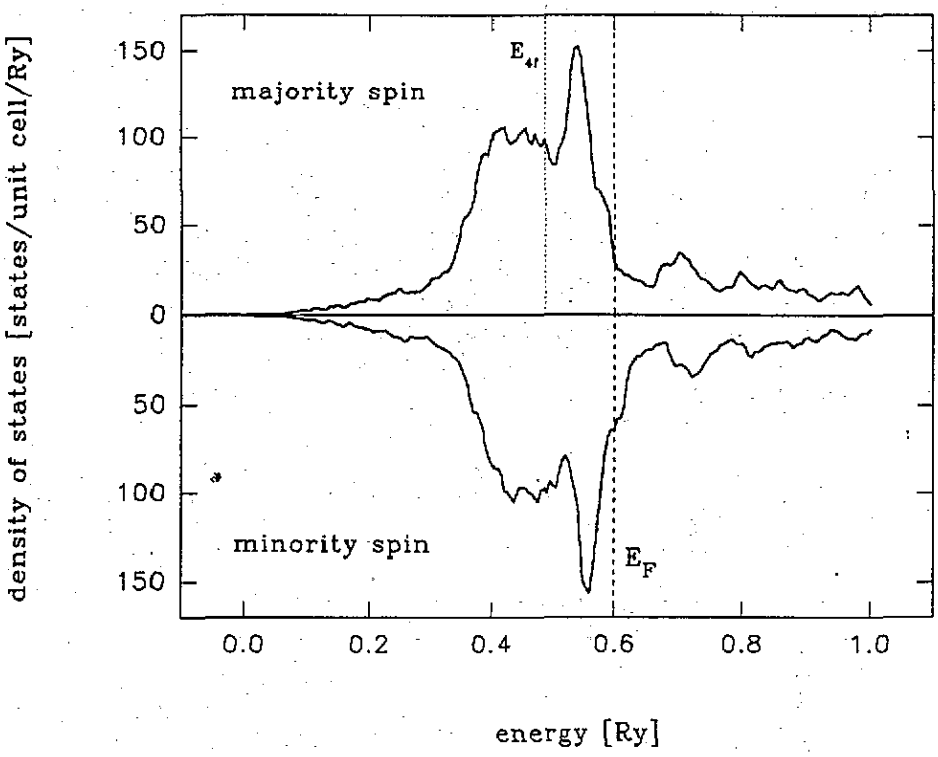

Figure 1. The DOS of valence states for the SP-B case. The position of the Fermi level E_F is denoted by the broken line. The dotted line marks the 4f level E_{4f}.

energy (from 0.65 to 1.0 Ryd) originate from Pr 5d states. The 4f level is situated 0.11 Ryd (1.5 eV) below the Fermi level. For the SP-A case the DOS is very similar to this in figure 1, but the shift of majority and minority spin DOS curves is smaller.

The total density of states at the Fermi level is $N_A(E_F) = 120$ for the SP-A case and $N_B(E_F) = 87$ for the SP-B case (both values in the units of states Ryd^{-1}/unit cell). Using the well known formula

$$\gamma = \tfrac{1}{3}\pi^2 k_B^2 N(E_F) \tag{2}$$

we can estimate the linear constant in the electronic contribution γT (T is the temperature) to the specific heat as $\gamma_A = 21$ mJ mol^{-1} K^{-2} and $\gamma_B = 15$ mJ mol^{-1} K^{-2}. These values are rather smaller than the experimental one of 40 mJ mol^{-1} K^{-2} [16].

3. Crystal field parameters

The Hamiltonian describing the behaviour of the Pr^{3+} ion in the hexagonal crystal field has the form:

$$\hat{H}_{cf} = B_{20}\hat{O}_{20} + B_{40}\hat{O}_{40} + B_{60}\hat{O}_{60} + B_{66}\hat{O}_{66} \tag{3}$$

where $\hat{O}_{LM}$ are Stevens operators and B_{LM} CFPs. CFPs were calculated using the simple relation [4]

$$B_{LM}/\alpha_L = \int_0^{R_{mt}} \beta_{LM} |R_{4f}(r)|^2 V_{LM}(r) r^2 \, dr \tag{4}$$

where α_L are Stevens factors [17], β_{LM} are coefficients related to $Y_{LM} \rightarrow \hat{O}_{LM}$ conversion [17], R_{4f} is the radial part of the 4f wave function and R_{mt} is the muffin-tin radius. V_{LM} is the LM component of either the Coulomb or the total self-consistent potential.

In order to determine how different regions of crystal contribute to CFPs, we have performed the decomposition of CFPs (calculated from the Coulomb potential) into the on-site and off-site contributions. The on-site contribution is calculated using the density inside the Pr muffin-tin sphere. Then, the off-site contribution is simply given as the complement to the whole value calculated using (4).

Table 1. The results of the CFP calculation together with the experimental values. CFPs are calculated using the Coulomb and total potentials. The on-site and off-site contributions are also given. See the text for the explanation of the symbols SP, NSP, A and B. Values of CFPs are in units of K.

	B_{20}/α_2	B_{40}/α_4	B_{60}/α_6	B_{66}/α_6
Calculation				
NSP				
on-site	−1889	10	−1.3	−41
off-site	1000	−46	5.6	252
Coulomb	−889	−36	4.3	211
total	−666	−39	6.1	261
SP-A				
on-site	−1906	9	−1.4	−43
off-site	1074	−49	6.0	280
Coulomb	−832	−40	4.6	237
total	−593	−42	6.7	293
SP-B				
on-site	−1817	−8	−0.6	−18
off-site	1095	−49	5.6	269
Coulomb	−722	−57	5.0	251
total	−499	−53	6.1	279
Experiment [8]	−282	−63	14	495

Table 1 shows the results of the CFP calculation. For comparison experimental data from [8] are also given.

In the case of the most significant parameter B_{20}, the calculated values are apparently larger (in magnitude) than the experimental one. The influence of the exchange–correlation potential is significant, approximately 30% of the value calculated using the Coulomb potential only. The results presented are in contradiction with the conclusion of Richter *et al* [6] that the exchange–correlation contribution may be neglected. In figure 2 the radial dependence of B_{20} integrands for the Coulomb and exchange–correlation contributions to B_{20} are plotted. As we can see from this figure, the exchange–correlation contribution cannot be neglected, but the region outside the Pr muffin tin seems to contribute, too. The

integration outside the muffin-tin sphere is difficult to perform because the 4f radial wave function is not well defined in this region. In the case of the rare earth metals studied by us [4] this problem did not appear and the exchange–correlation contribution is properly defined. The on-site and off-site contributions agree with values reported by Daalderop *et al* [3] for $GdCo_5$.

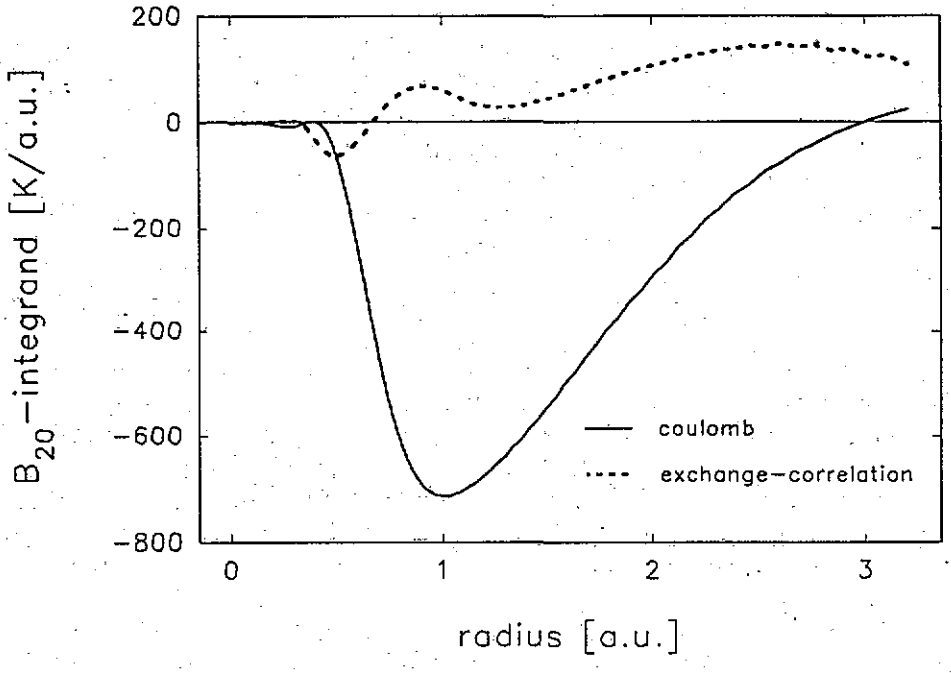

Figure 2. The radial dependence of B_{20} integrands for the NSP case. The full curve represents the Coulomb contribution to B_{20} and the broken curve the exchange–correlation one. The muffin-tin radius is 3.2 au.

For the B_{40} parameter, the agreement with the experiment is better than for the B_{20} one. In this case the influence of the exchange–correlation potential is small. We should note here that this is not true for the above mentioned case of rare earth metals [4] and the cubic materials with the CsCl structure investigated in [7].

Calculated values of the sixth-order parameter B_{60} also reproduce the experiment satisfactorily. The influence of the exchange–correlation potential is apparent. Calculation of the B_{66} parameter gives values that are significantly smaller than the experimental one. The off-site contribution dominates in this case.

We conclude that our method of calculation of B_{20} leads to deviation by a factor of 2–3 from the experiment. This agrees with analogous conclusions of Daalderop *et al* [3] and Richter *et al* [6]. The reason for this discrepancy might lie in the hybridization of the f electrons with the valence electrons, which was neglected in all these calculations. On the other hand, we can see that the B_{20} parameter is sensitive to the type of calculation performed, i.e. to the details of electronic bands and their occupations—in contrast to higher-order CFPs. The on-site contribution (which reflects electronic structure) is large for the B_{20} case and its magnitude even predominates over the off-site one. The off-site contribution is due to the charges outside the 4f region which implies its small sensitivity to electronic

structure details. For other CFPs the off-site contribution dominates and for this reason they are not so heavily influenced. These facts are supported by experimental findings (see, e.g., [18]) and B_{20} seems to be the most sensitive parameter with respect to the change of experimental conditions.

4. Electric field gradient

In $PrNi_5$, there are three contributions to the EFG at the Pr nucleus site [9]. First, there is the contribution originating from 4f electrons, which can be estimated if the state of the 4f shell is known. Second, band electrons also contribute to the EFG. This contribution follows from band structure. Third, there is the pseudoquadrupole contribution [17] arising from magnetic hyperfine interaction.

We denote these contributions as P_1, P_2 and P_3 in the order given above. We will work in the energetic scale. First, P_1 is given by the formula

$$P_1/h = -[3e^2Q\langle r^{-3}\rangle/4I(2I-1)]\alpha_2\langle\Psi|3\hat{J}_z^2 - J(J+1)|\Psi\rangle \tag{5}$$

where $Q = -0.059$ b is the quadrupole moment of ^{141}Pr nucleus [19], $\langle r^{-3}\rangle = 5.0$ au^{-3} was obtained using Pr atomic 4f wave functions, $|\Psi\rangle = 1/(\sqrt{2})(|+3\rangle - |-3\rangle)$ is the ground state of the Pr^{3+} ion and other symbols have their usual meaning. We obtained $P_1/h = -0.8$ MHz, which agrees with the value of -0.7 MHz given in [9].

Second, the band electron contribution was determined using the method of Blaha *et al* [20] and the results are given in table 2 for different types of calculation. Third, we used the value $P_3 = 4.0$ MHz determined in [9].

Table 2. The results of the EFG calculation. P_2 is the band electron contribution. The resulting P value was calculated using $P_1/h = -0.8$ MHz and $P_3/h = 4.0$ MHz.

Calculation	P_2/h (MHz)	P/h (MHz)
NSP	−0.7	2.5
SP-A	−0.6	2.6
SP-B	−1.1	2.1

The total EFG is given by the sum of all contributions as is shown in table 2. For the experimental value [9] only the magnitude of 0.6 MHz is known. Though our results are several times greater than the experimental one, we predict the sign of the EFG.

5. Magnetic moments

Spin-polarized band structure calculations yield values of magnetic moments automatically. We obtained simply the values of moments localized on different sites of crystal and also the total ones. Table 3 collects the results of our calculations. The total energy (per unit cell) for each type of calculation performed is also given.

At first sight, these results are surprising. The energy of the crystal when the moments of Pr and Ni are parallel is lower than that for antiparallel moments. This contrasts with the RCo_5 (R = rare earth) compounds where 3d moments of Co and 4f moments are always antiparallel. Moreover, the energy of antiparallel orientation is higher than the energy when

Table 3. Magnetic moments (in units of μ_B) calculated for both spin-polarized cases. The on-site and total (per unit cell) moments are given. Values for Pr do not include the 4f electron contribution. In the case of SP-A the total magnetic moment value oscillates around zero with deviations of about $\pm 0.01\ \mu_B$. Ni(1) and Ni(2) are two crystallographically non-equivalent sites of Ni. The total energy (in units of Ryd) for all calculations performed is also given.

Calculation	Pr	Ni(1)	Ni(2)	Total	E_{tot}
NSP	—	—	—	—	−33 654.301
SP-A	0.08	−0.01	−0.01	∼0	−33 654.283
SP-B	0.02	+0.22	+0.20	1.34	−33 654.307

the spin polarization is not considered. The values of Ni magnetic moments in the SP-B case seem to be larger than the limit imposed by [8]. On the other hand, the small Ni moments, as calculated in the second spin-polarized case A, cannot be measured.

One point should be discussed now. There is a possibility that the lattice parameters given in [11] are not quite correct. We have not inspected the dependence of the total energy of the system studied on the lattice parameters. In general, the total energy as a function of lattice parameters and magnetization has several minima. This function should be studied in detail (using the above mentioned fixed spin moment method) to decide the question about the ground state of $PrNi_5$, which is a difficult task with respect to the time demands. We have performed a similar investigation for $SmCo_5$ [14] and we have obtained the correct ground state and correct values of magnetic moments, the latter in good agreement with the calculation of Richter *et al* [6].

Acknowledgments

We are grateful to Dr J Šebek who initiated our work. Thanks are due to the computing centre of the Insitute of Physics where part of the calculation was performed on the CRAY Y-MP EL computer. This work was partially supported by the Charles University Grant Agency (Prague), Project No 288. We thank Dr M Diviš for valuable discussions.

References

[1] Xue-Fu Zhong and Ching W Y 1989 *Phys. Rev.* B **39** 12 018
[2] Coehoorn R 1991 *J. Magn. Magn. Mater.* **99** 55
[3] Daalderop G H O, Kelly P J and Schuurmans M F H 1992 *J. Magn. Magn. Mater.* **104–7** 737
[4] Novák P and Kuriplach J 1992 *J. Magn. Magn. Mater.* **104–7** 1499; 1993 *Physics of Transition Metals (Proc. ICPTM '92, Darmstadt)* vol 2, ed P M Oppeneer and J Kübler (Singapore: World Scientific) p 609
[5] Humler K, Liebs M, Beuerle T and Fähnle M 1993 *Physics of Transition Metals (Proc. ICPTM '92, Darmstadt)* vol 2, ed P M Oppeneer and J Kübler (Singapore: World Scientific) p 710
[6] Richter M, Oppeneer P M, Eschrig H and Johansson 1992 *Phys. Rev.* B **46** 13 919
[7] Diviš M and Kuriplach J 1993 *Physica* B **183** 25
[8] Amato A, Bührer W, Grayevsky A, Gygax F N, Furrer A, Kaplan N and Schenck A 1992 *Solid State Commun.* **82** 767
[9] Kaplan N, Williams D LI and Grayevsky A 1980 *Phys. Rev.* B **21** 899
[10] Blaha P, Schwarz K, Sorantin P and Trickey S B 1990 *Comput. Phys. Comm.* **59** 399
[11] Wernick J and Geller S 1959 *Acta Crystallogr.* **12** 662
[12] The form of potential is from von Barth U and Hedin L 1972 *J. Phys. C: Solid State Phys.* **5** 1629, and the parameters of this potential are from
Janak J F 1977 *Phys. Rev.* B **16** 255
[13] Hedin L and Lundqvist B I 1971 *J. Phys. C: Solid State Phys.* **4** 2064

[14] Novák P and Kuriplach J 1993 *Proc. EMMA'93 (Košice); IEEE Trans. Magn.* at press
[15] Schwarz K and Mohn P 1984 *J. Phys. F: Met. Phys.* **14** L129
[16] Ott H R, Andres K, Bucher E and Maita J P 1976 *Solid State Commun.* **18** 1303
[17] Abragam A and Bleaney B 1970 *Electron Paramagnetic Resonance of Transition Ions* (Oxford: Clarendon)
[18] Diviš M 1991 *PhD Thesis* Prague
[19] Lederer C M and Shirley V S (eds) 1978 *Table of Isotopes* (New York: Wiley) p A-55
[20] Blaha P, Schwarz K and Herzig P 1985 *Phys. Rev. Lett.* **54** 1192